

# Inhibition of fibroblast proliferation in cardiac myocyte cultures by surface microtopography

Samuel Y. Boateng,<sup>1</sup> Thomas J. Hartman,<sup>1</sup> Neil Ahluwalia,<sup>1</sup>  
Himabindu Vidula,<sup>1</sup> Tejal A. Desai,<sup>2</sup> and Brenda Russell<sup>1</sup>

<sup>1</sup>Department of Physiology and Biophysics, University of Illinois at Chicago, Chicago, Illinois 60612-7342; and  
<sup>2</sup>Department of Biomedical Engineering, Boston University, Boston, Massachusetts 02215

Submitted 13 January 2003; accepted in final form 11 March 2003

**Boateng, Samuel Y., Thomas J. Hartman, Neil Ahluwalia, Himabindu Vidula, Tejal A. Desai, and Brenda Russell.** Inhibition of fibroblast proliferation in cardiac myocyte cultures by surface microtopography. *Am J Physiol Cell Physiol* 285: C171–C182, 2003. First published April 2, 2003; 10.1152/ajpcell.00013.2003.—Cardiac myocyte cultures usually require pharmacological intervention to prevent overproliferation of contaminating nonmyocytes. Our aim is to prevent excessive fibroblast cell proliferation without the use of cytostatics. We have produced a silicone surface with 10- $\mu$ m vertical projections that we term “pegs,” to which over 80% of rat neonatal cardiac fibroblasts attach within 48 h after plating. There was a 50% decrease in cell proliferation by 5 days of culture compared with flat membranes ( $P < 0.001$ ) and a concomitant 60% decrease ( $P < 0.01$ ) in cyclin D1 protein levels, suggesting a G<sub>1</sub>/S<sub>1</sub> cell cycle arrest due to microtopography. Inhibition of Rho kinase with 5 or 20  $\mu$ M Y-27632 reduced attachment of fibroblasts to the pegs by over 50% ( $P < 0.001$ ), suggesting that this signaling pathway plays an important role in the process. Using mobile and immobile 10- $\mu$ m polystyrene spheres, we show that reactive forces are important for inhibiting fibroblast cell proliferation, because mobile spheres failed to reduce cell proliferation. In primary myocyte cultures, pegs also inhibit fibroblast proliferation in the absence of cytostatics. The ratio of aminopropeptide of collagen protein from fibroblasts to myosin from myocytes was significantly reduced in cultures from pegged surfaces ( $P < 0.01$ ), suggesting an increase in the proportion of myocytes on the pegged surfaces. Connexin43 protein expression was also increased, suggesting improved myocyte-myocyte interaction in the presence of pegs. We conclude that this microtextured culture system is useful for preventing proliferation of fibroblasts in myocyte cultures and may ultimately be useful for tissue engineering applications in vivo.

tissue engineering; cell culture; cell cycle

---

IN PRIMARY CULTURES of the neonatal heart, cell interactions between myocytes and nonmyocytes have a profound effect on myocyte behavior by both autocrine and paracrine signaling pathways (21). Therefore, retention of the physiological numbers of nonmyocytes in cell culture is highly desirable. Terminally differentiated myocytes do not proliferate, but other cells in the

primary culture do. Unfortunately, excessive proliferation of the nonmyocytes occurs in the serum media necessary for myocyte viability. Researchers often restrict cell division by using cytostatic drugs such as cytosine  $\beta$ -D-arabino-furanoside (AraC) (15), but these can induce apoptosis in many cell types (12). Thus the elimination of such drugs from these cultures would be beneficial.

A long-term goal of our group is to use biotechnological approaches to recapitulate both the architecture and surface chemistry (1, 20), in vitro, to obtain a more biological phenotype in culture. In other studies, cells have been embedded into extracellular matrix proteins in an attempt to recapitulate some of their native environment. For example, hepatocytes can be maintained in culture for more than 40 days in a three-dimensional (3-D) collagen gel sandwich compared with only 1 wk on a conventional collagen monolayer (9). Fibroblasts display different expression and localization of integrin and cytoskeletal components in tissue-derived 3-D matrices and 3-D collagen lattices compared with the conventional 2-D culture systems (7).

Microtextured surfaces have also been used to generate 3-D environments for cells in culture. These surfaces, formed through photolithography and microfabrication, have been shown to alter the behavior of many cells types (8, 13, 32). The spatial dimensions of the surface topography play a critical role in regulating cell behavior (32, 35).

In addition to providing a more 3-D environment for cell attachment and growth, we have found that microtopography with 10- $\mu$ m vertical silicone projections also reduces fibroblast cell proliferation. We explore some of the mechanical and signaling mechanisms by which microtopography affects the cell cycle in cultured cardiac fibroblasts from newborn rats. The mechanism of contact inhibition is usually thought to be initiated and mediated by the interaction of cell surface molecules with adjacent cells (25). Integrins in focal adhesions play an important part in contact and mechanosensory processes (10). The force-induced assembly of the focal adhesions can activate a number of signaling pathways, including the Rho GTPase family, that

---

Address for reprint requests and other correspondence: B. Russell, Dept. of Physiology and Biophysics (M/C 901), Univ. of Illinois at Chicago, 835 S. Wolcott Ave., Chicago, IL 60612-7342 (E-mail: Russell@uic.edu).

---

The costs of publication of this article were defrayed in part by the payment of page charges. The article must therefore be hereby marked “advertisement” in accordance with 18 U.S.C. Section 1734 solely to indicate this fact.

affect cell adhesion, differentiation, proliferation, and survival (11). We have taken advantage of this inhibitory phenomenon to decrease fibroblast overgrowth in cardiac myocyte culture without the use of chemical cytostats.

In this study, we cultured cells on microtopography with vertical silicone projections that we have termed “pegs” and show altered gene expression and a reduction of fibroblast cell proliferation more like that seen *in vivo*. We show, by our use of mobile and immobile chemically inert spheres, that reactive forces on the attached cells in association with the vertical topography produce these effects in the absence of an extracellular matrix. Our results show that the interaction with the microtopography is mediated, at least in part, through the Rho signal transduction pathway. Furthermore, we show that microtextured membranes reduce nonmyocyte proliferation in myocyte cultures, thereby removing the unwanted side effects of pharmacological intervention in these cells.

## MATERIALS AND METHODS

**Polymeric microtextured membranes.** Microtextured polymeric membranes were fabricated by using the technique of photolithography, in which silicon wafers are used as templates to reproduce complimentary microscale topographies on the desired polymers. Silicone membranes were fabricated as described previously (8) to produce 10- $\mu\text{m}$  pegs projecting from the flat surface of the culture dish (Fig. 1). Membranes were sterilized in 70% ethanol for at least 1 h, rinsed, and plated with fibroblasts. Some cells were grown on membranes produced from flat parylene to assess the effects of any trace chemicals on the otherwise inert silicone. Some membranes were coated with laminin before myocyte plating to assess surface chemistry. For experiments with fibroblasts, the silicone membranes were not coated with matrix, but for myocytes, membranes were coated with 20  $\mu\text{g}/\text{ml}$  laminin (Sigma) in Dulbecco's modified Eagle's medium (DMEM) Nutrient Mixture F-12 Ham (Sigma) for 5 h before plating.

**Myocyte and fibroblast cell cultures.** Hearts were removed from 1- to 2-day-old neonatal Sprague-Dawley rats and placed in Moscona's saline (136.8 mM NaCl, 28.6 mM KCl, 11.9 mM  $\text{NaHCO}_3$ , 9.4 mM glucose, and 0.08 mM  $\text{NaH}_2\text{PO}_4$ , pH 7.4) on ice. The atria were removed and washed several times with cold Moscona's and then with cold KRB I [118.4 mM NaCl, 2.4 mM  $\text{MgSO}_4$ , 4.7 mM KCl, 23.8 mM  $\text{NaHCO}_3$ , 1.5 mM  $\text{KH}_2\text{PO}_4$ , 11.1 mM glucose, 1 mg/ml BSA fraction V, 1 m/ml penicillin G/streptomycin (Sigma), and phenol red, gassed with 5%  $\text{CO}_2$ , pH 7.4] and minced with dissecting

scissors. The cells were dissociated at 37°C in a shaking water bath for 10-min periods at 50 oscillations/min with a collagenase type 2 at 0.42 mg/ml (Worthington Biochemical) in KRB II [118.4 mM NaCl, 2.4 mM  $\text{MgSO}_4$ , 4.7 mM KCl, 23.8 mM  $\text{NaHCO}_3$ , 1.5 mM  $\text{KH}_2\text{PO}_4$ , 11.1 mM glucose, 20 mg/ml BSA fraction V, 1 m/ml penicillin G/streptomycin (Sigma), and phenol red, gassed with 5%  $\text{CO}_2$ , pH 7.4]. During the digestion, triturating the tissue through a cannula/syringe mechanically disrupted the tissue. The cells released after the first digestion were discarded (fibroblast and debris-rich mixture), whereas the cells from subsequent digestions were added to 25 ml of KRB II and kept on ice. After final collection, the cells were pelleted by centrifugation (5,000 rpm for 6 min at room temperature). The supernatant was discarded, and cells were resuspended in complete medium [DMEM Nutrient Mixture F-12 Ham without L-glutamine (Sigma), standard amino acid concentrations plus palmitic (2.56 mg/l) and linoleic (0.84 mg/l) fatty acids, penicillin G/streptomycin (1 mg/ml) and gentamicin (50mg/l)] and then filtered through a metal sieve to filter out large material. The resulting cell mixture was preplated for 1 h in a 37°C  $\text{CO}_2$  incubator to plate out the fibroblasts. The remaining enriched myocytes were then plated at high density (1,000 cells/ $\text{mm}^2$ ) either with or without 18  $\mu\text{M}$  AraC.

Complete medium was then added to the preplated fibroblasts, and they were then cultured for another 2 days before being passaged for fibroblast experiments. Primary myocytes were obtained from neonatal rats according to Institutional Animal Care and Use Committee and National Institutes of Health Guidelines for the Care and Use of Laboratory Animals (NIH publication 85-23, Revised 1985).

For the fibroblast experiments, cell number was assessed by cytometric counting after 1, 2, and 5 days following trypsinization. Cell number on each surface was assessed by averaging the counts from four dishes. Comparisons between surfaces and days were made by normalizing all other conditions to the *day 1* flat dish average, which was expressed as 100%.

**Cell attachment and proliferation.** To determine the degree of fibroblast cell attachment to 10- $\mu\text{m}$ -high pegs, cells were initially plated at a density of 100 cells/ $\text{mm}^2$  on flat or microtextured membranes in 35-mm dishes. Digital images were taken of the cells at various time points after plating. For each time point, cells were counted from five micrographs randomly taken. A cell was considered attached when one of its extensions terminated on a peg. As a control, micrographs were taken from cells on a flat dish, and attachments were assessed by means of “virtual pegs” drawn on an overlay. The number of cells that would have randomly attached to a virtual peg was assessed and compared with the cells actually attached from pegged membranes. The percentage of cells attached was measured over 5 days, and cell number per unit area was measured from micrographs and confirmed by cytometric counts after trypsinization.

**Microtopography and cell proliferation.** The microtopography of polystyrene petri dishes was altered by the addition of 10- $\mu\text{m}$  polystyrene microspheres. Spheres were either allowed to remain free in the dish (mobile) or were immobilized to the surface (immobile) by being heated to 80°C. Digital phase microscopy was used to determine fibroblast morphology. The cells were cultured for 24 h. Cell number per unit area was measured from micrographs and confirmed by cytometric counts after trypsinization.

**Total DNA measurements.** DNA was isolated from myocytes by using the DNeasy tissue kit (Qiagen) after 4 days of culture. DNA was measured spectrophotometrically and expressed as micrograms per 35-mm culture dish.

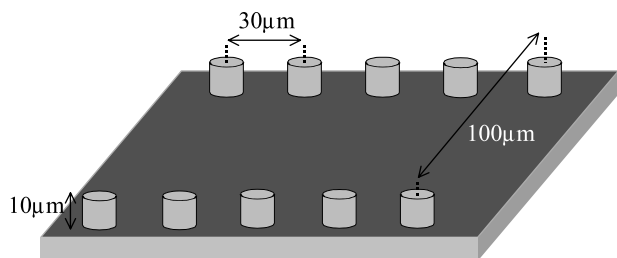


Fig. 1. Diagram of a silicone surface with microtopography showing 10- $\mu\text{m}$ -high pegs in a rectangular pattern with 30- and 100- $\mu\text{m}$  spacing between them.

*Protein analysis by Western blotting.* Protein preparations, Western blots, and their analyses were performed as described previously (2). We measured vimentin (Santa Cruz Biotechnology), actin (Oncogene Research Products),  $\beta_1$ -integrin (Research Diagnostics), and cyclin D<sub>1</sub> (Santa Cruz Biotechnology) in fibroblasts. The expression of connexin43

(Transduction Laboratories), myosin heavy chain [Developmental Studies Hybridoma Bank (DSHB)], and the amino-propeptide of collagen (DSHB) was measured in myocyte/fibroblast cultures. Peroxidase-conjugated secondary antibodies of donkey anti-goat, donkey anti-mouse, and donkey anti-rabbit (Research Diagnostics) were used. Cyclin D<sub>1</sub> and

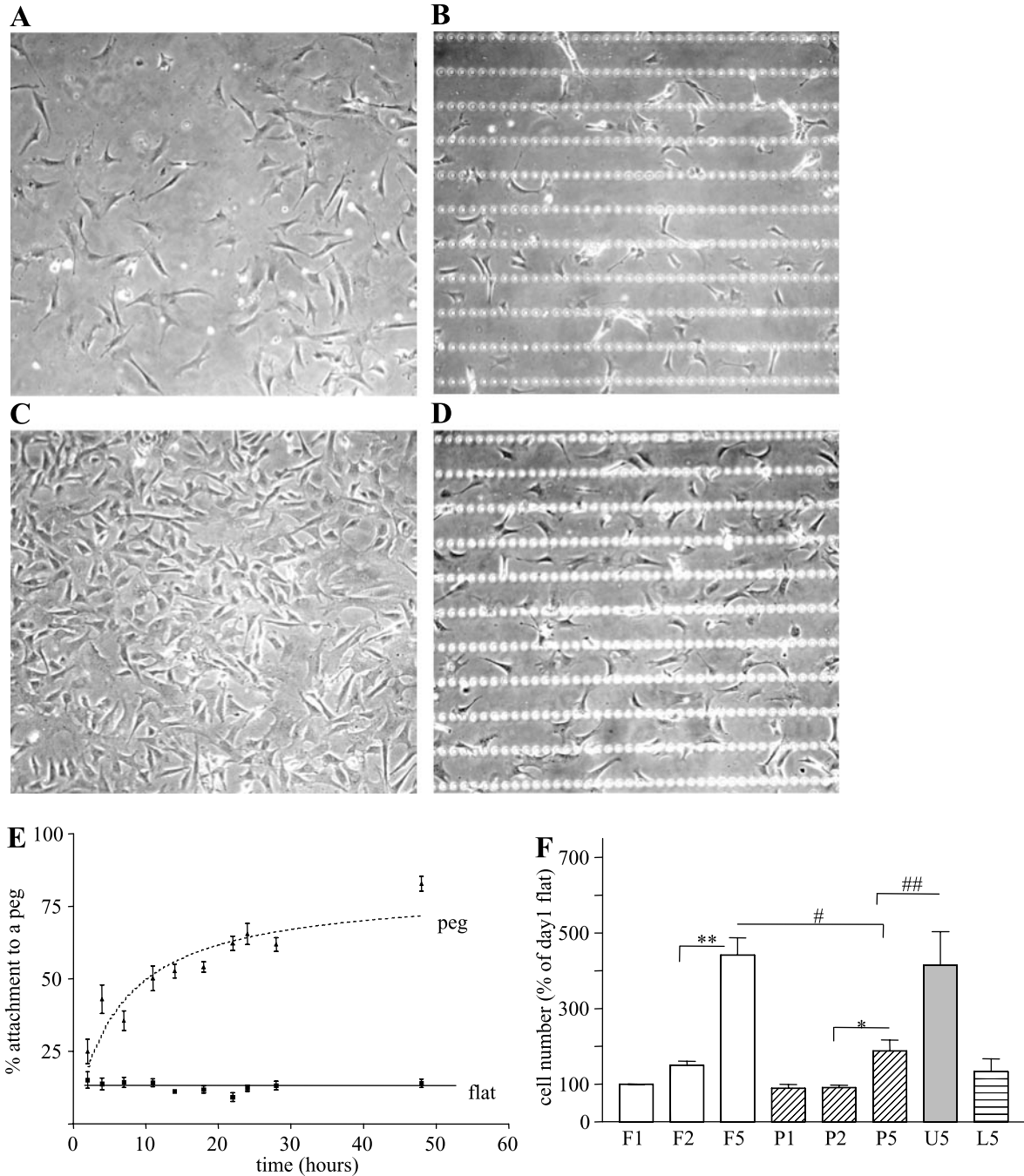


Fig. 2. Cell attachment and proliferation on flat or microtextured silicone surfaces. *A–D*: phase images show fibroblasts after 2 and 5 days of culture. *A*: 2 days on flat silicone membranes. *B*: 2 days on silicone textured with rows of 10- $\mu$ m pegs. *C*: 5 days on flat silicone membranes. *D*: 5 days on silicone textured with rows of 10- $\mu$ m pegs. *E*: time course of cellular attachment to pegs over a 48-h period. For flat surfaces, superimposed “virtual pegs” measured “attachment” over the same period. *F*: time course of cell proliferation over a 5-day period on both flat and pegged surfaces. Cells were cultured on flat untextured membranes (F), pegged membranes (P), flat silicone made from untextured parylene (U), and pegged membranes coated with laminin protein (L); numbers refer to the number of days of culture. Plotted values are means  $\pm$  SE;  $n = 8$  cultures in all groups. **\*\*** $P < 0.001$ , F2 vs. F5. **#** $P < 0.001$ , F5 vs. P5. **\*** $P < 0.001$ , P2 vs. P5. **##** $P < 0.05$ , P5 vs. U5.

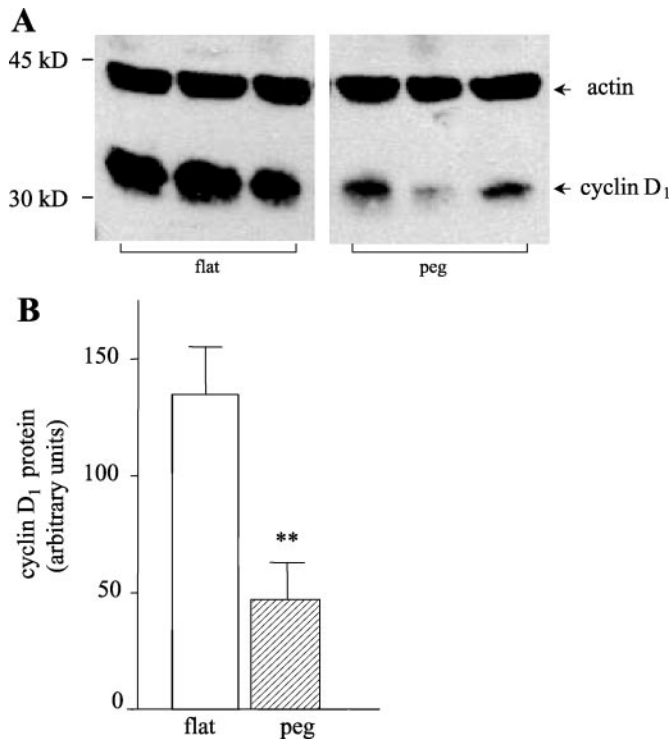


Fig. 3. *A*: Western blots of cyclin D<sub>1</sub> and actin protein of fibroblasts from flat and pegged membranes. *B*: relative changes in cyclin D<sub>1</sub> protein abundance in fibroblasts plated on flat and pegged surfaces. Values are means  $\pm$  SE;  $n = 6$  cultures. Cyclin D<sub>1</sub> protein is significantly reduced on pegged membranes compared with flat ones (\*\* $P < 0.01$ ). Actin protein was used as an internal control because it was unchanged in both groups.

$\beta_1$ -integrin were measured from fibroblasts after 2 days in culture on flat and pegged membranes and before the cells on the flat membranes became confluent. In myocytes, protein expression was assessed after 4 days of culture.

**Immunocytochemical staining.** Immunostaining was performed as previously described (28) by using anti-focal adhesion kinase (FAK) antibody (Upstate Biotechnology), anti- $\beta$ -tubulin (Sigma), anti-myosin (MF-20; DSHB), anti-amino-peptide of collagen (SP1.D8; DSHB), and appropriate fluorescently labeled secondary antibodies. Counterstaining for actin was done by using either Alexa Fluor 488 phalloidin (Molecular Probes) or rhodamine-phalloidin (Molecular Probes). The concentration of rhodamine-conjugated phalloidin was kept relatively low (1 in 1,000) so that nonstriated actin staining was minimal. This provided a way of distin-

guishing between fibroblasts and myocytes. Membranes were then mounted on glass slides, and Vectashield with 4',6-diamidino-2-phenylindole (DAPI; Vector Laboratories) was added as a nuclear stain and anti-fade reagent. Stains were visualized with a fluorescence microscope (Nikon Microphot-FXA), and images were digitally captured with a Spot RT Color Camera (Diagnostic Instruments).

**Cell attachment and motility with Rho kinase inhibition.** To examine the role of focal adhesions in the cell attachment to pegged microtopography, 5 or 20  $\mu$ M Y-27632, a Rho kinase inhibitor drug, was used on cardiac fibroblasts. For these studies, cells were again plated at a density of 100 cells/mm<sup>2</sup>. The concentration of Y-27632 used to inhibit Rho kinase was 100 times lower than that required to affect the cell cycle in fibroblasts (24). The drug was added 6 h after plating, and the medium with drug was changed once after 24 h. Photographs of cells with and without drug treatment were taken as described above at 7, 24, and 48 h after plating and attachment of fibroblast cells was assessed (i.e., at 1, 18, and 42 h of drug treatment). The velocity of cell motility was assessed by observing cells under phase microscopy with time-lapse video and was recorded in real time. To measure cell crawling velocity (in  $\mu$ m/min), a single cell was observed for six 10-min intervals totaling 1 h. The distance that the nucleus traveled over 10 min was then averaged. Each  $n$  value represents one separate week of culture and contains an average of 5–7 cells per culture. This velocity measurement was repeated after application of Y-27632 for 2 h following an initial 6 h of plating, namely, at 8 h after plating.

Cell crawl velocities were also measured after attachment to pegs. Attachment to a peg was deemed to have taken place when a cell extension was in contact with the peg and the nucleus had begun to move toward the peg. The velocity of the cell was once again determined as described above.

**Statistical analysis.** Data are presented as means  $\pm$  SE. Sample number ( $n$ ) was defined as a separate culture performed at a different time from different animals. Data groups were compared using one-way ANOVA followed by a Turkey-Kramer multiple comparisons test. Significance was taken at  $P < 0.05$ .

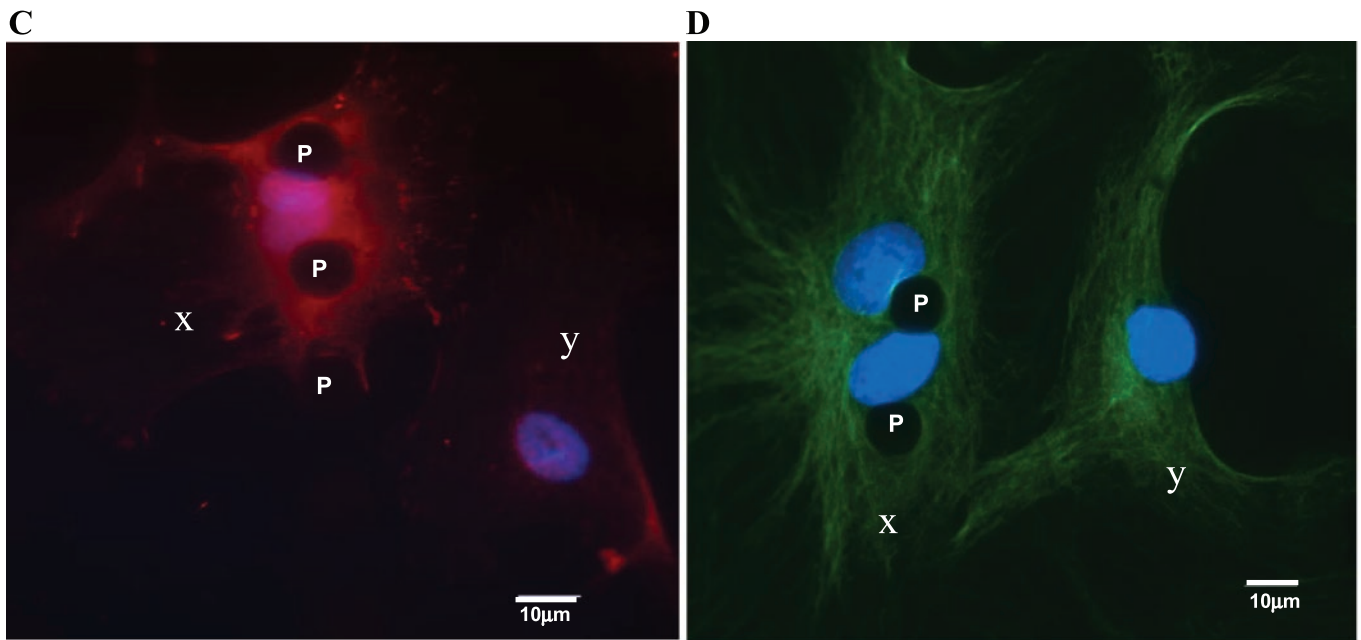
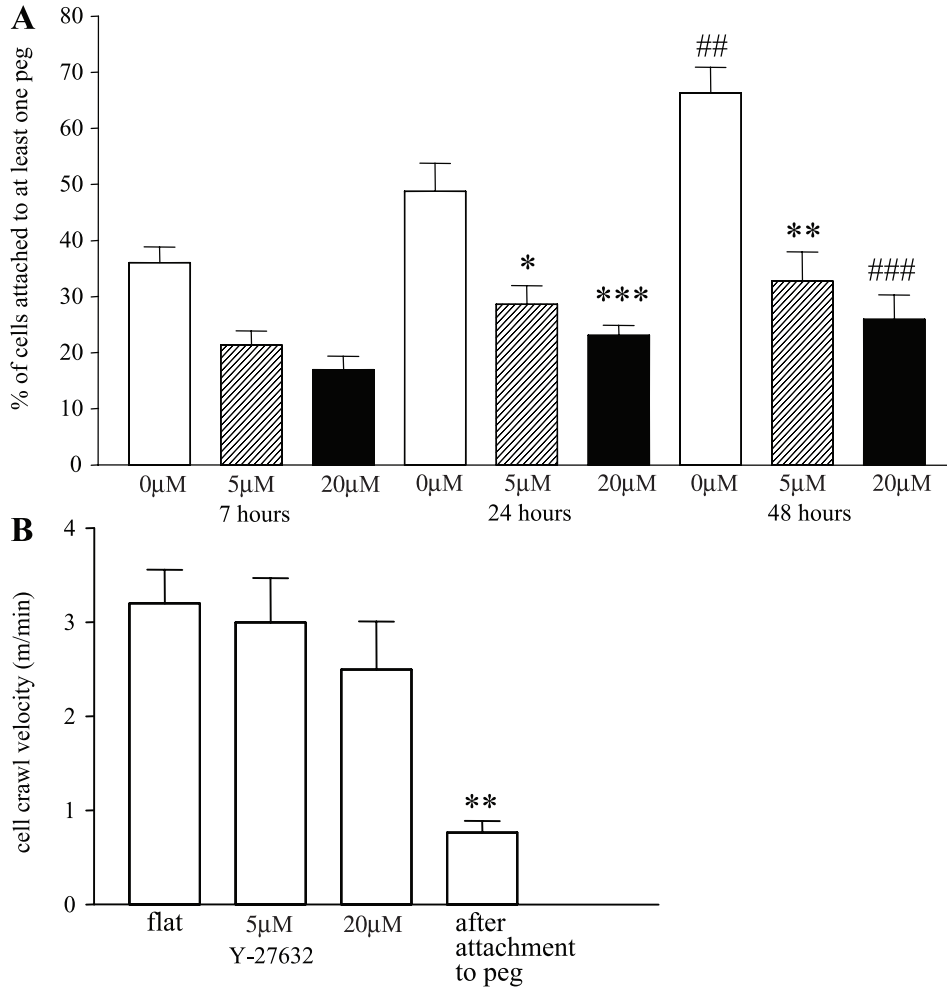
## RESULTS

**Cell proliferation and microtopography.** Cells were plated on 10- $\mu$ m pegged silicone membranes with a microarchitecture of micropegs providing a vertical surface for the attachment of cells (Fig. 1). Figure 2, *A* and *B*, shows fibroblasts after 48 h of culture on flat and pegged membranes, respectively. At this time, cell number was similar between the two surfaces. After 5 days of culture, there were fewer cells on membranes

Fig. 4. *A*: Rho kinase inhibition and cellular attachment to microtopography. In the absence of Y-27632, there was a significant increase in cellular attachment to vertical pegs (as in Fig. 2C) from 7 h (0  $\mu$ M drug) to 48 h (0  $\mu$ M drug) (## $P < 0.001$ ). However, with 5 or 20  $\mu$ M Y-27632, there was no significant increase in cellular attachment with time. There is a significant difference with decreased attachment to pegs at 24 h ( $*P < 0.05$ ) and at 48 h (\*\* $P < 0.001$ ) with 5  $\mu$ M Y-27632; the same is also true at the respective times (\*\*\* $P < 0.001$  and ### $P < 0.001$ ) with 20  $\mu$ M Y-27632. Values are means  $\pm$  SE;  $n = 6$  cultures. *B*: effect of Rho kinase inhibition and microtopography on cell motility using time-lapse videography. Rho kinase inhibition with Y-27632 at concentrations of 5 or 20  $\mu$ M had no effect on cell motility. However, the velocity of cell motility was significantly reduced after attachment to pegs (\*\* $P < 0.001$ ). Values are means  $\pm$  SE;  $n = 3$  cultures. *C*: immunofluorescence of fibroblasts stained for focal adhesion kinase (FAK; red) and 4',6-diamidino-2-phenylindole (DAPI; blue). Cell *x* is attached to 3 pegs (P indicates the position of each peg); cell *y* is growing on a flat area of the membrane and is not attached to a peg. There is an intense accumulation of FAK protein in the cell near a peg compared with the cell on the adjacent flat surface. *D*: immunofluorescence of fibroblasts labeled for tubulin (green) and nuclei (DAPI; blue). Cells *x* are attached to 2 pegs, and the nuclei are drawn toward them and are distorted. Cell *y* is unattached to any pegs, and the nucleus is undistorted.

with pegs (Fig. 2, C and D). The time course of cellular attachment shows a steady increase in the number of cells that have attached to a peg over 48 h (Fig. 2E). Attachment increased from under 30% at 2 h to over

80% at 48 h. To assess whether this appearance was random, we compared scores taken by placing drawings of pegs on top of micrographs taken of cells grown on a flat dish. The number of cells that ended at the



location of virtual pegs was constant at  $\sim 12\%$  between 2 and 48 h. There was a steady increase in cell number over 5 days of culture on flat dishes, detected by counting from micrographs (Fig. 2F). However, there was a smaller increase in cell proliferation on pegged membranes over that period (Fig. 2F). By 5 days of culture, the cell number was twofold higher on flat membranes compared with pegged ones. These numbers were verified by trypsinization and cytometric cell counts (data not shown).

We ruled out any side effects due to residues of fabrication by growing cells on untextured silicone made from the same precursor template material (parlylene) as the microtextured membrane (Fig. 2F). After 5 days in culture, the number of fibroblasts on the parlylene-derived flat membranes did not differ significantly from that on the flat membranes made without parlylene. To test whether the effects of the pegged surface on cell proliferation would be observed in the presence of a layer of surface matrix, we also counted cells on laminin-coated membranes. Fibroblast cell number was not significantly different on *day 5* between the laminin-coated and uncoated pegged membranes (Fig. 2F).

**Fibroblast gene expression and microtopography.** To determine whether the inhibition of cell proliferation was being regulated at the level of the cell cycle, we measured cyclin D<sub>1</sub> levels in fibroblasts from flat and pegged surfaces. Measurements from fibroblasts were taken at 48 h, a time when cell density was low and cell number was comparable on both surfaces. On flat membranes, cells were in the logarithmic phase of cell proliferation. Examples of Western blots of cyclin D<sub>1</sub> along with total actin in the same samples are presented (Fig. 3A) and quantified (Fig. 3B). On flat membranes, fibroblasts expressed high levels of cyclin D<sub>1</sub>, indicating that the cells were actively dividing. However, there was a significant 65% decrease in cyclin D<sub>1</sub> levels from fibroblast cultures grown on pegged membranes after 48 h of culture compared with those on flat membranes. The ratio of  $\beta_1$ -integrin expression to actin was increased by 30% ( $P < 0.05$ ,  $n = 4$  cultures) on pegged membranes after 48 h of cultures (data not shown). Actin and vimentin protein expression assessed by Westerns remained unchanged between both groups (data not shown).

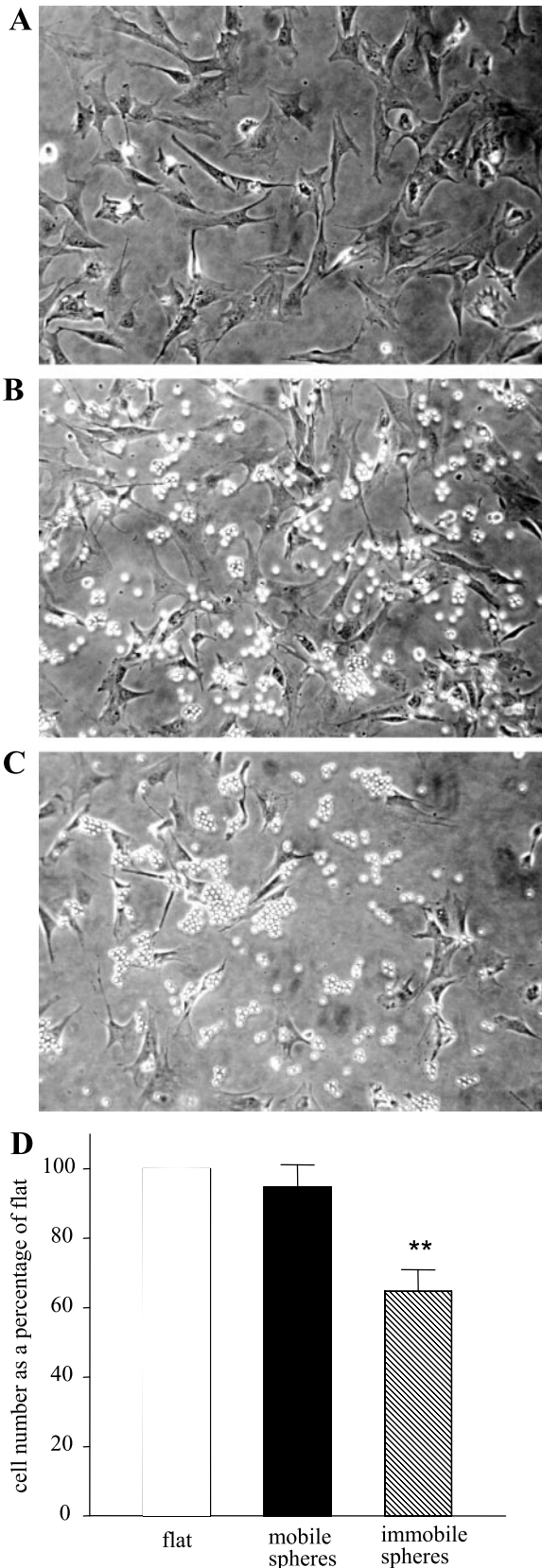
**Rho kinase and FAK and cell attachment to microtopography.** To examine the possible role of focal adhesions in the time-dependent increase in cellular attachment to pegs, we used the drug Y-27632 to inhibit Rho kinase. The concentrations chosen (5 and 20  $\mu\text{M}$ ) do not inhibit fibroblast cell proliferation (24). The effects of Rho kinase inhibition on cellular attachment to pegs are shown in Fig. 4A. In the absence of drug there is a steady and significant increase in the number of fibroblasts attached to pegs, and this rises to  $\sim 70\%$  after 48 h of plating, also shown in Fig. 2E. In contrast, cells exposed to either 5 or 20  $\mu\text{M}$  Y-27632 showed significantly lower cellular attachment at 7 h, after just 1 h of drug treatment. In the presence of Y-27632, there was no significant increase in cellular attachment over the

48-h period. After 48 h (and 42 h of drug treatment), the number of cells attached to pegs was less than half that of untreated cells.

To determine the effect of Rho kinase inhibition on fibroblast cell motility, we took time-lapse video microscopy of cells on flat surfaces in the presence of Y-27632. The results in Fig. 4B show that both 5 and 20  $\mu\text{M}$  concentrations of Y-27632 did not significantly alter the velocity of cell motility. Cell motility on the micropeg surfaces was also determined before and after attachment to pegs. When cells were unattached to the vertical pegs, the motility was similar to that on flat surfaces (data not shown). However, when a fibroblast encountered a peg, the velocity of its crawling was significantly decreased by  $\sim 75\%$ , ( $P < 0.01$ ). Thus attachment to vertical pegs significantly reduces fibroblast cell motility (Fig. 4B).

Immunocytochemical staining of fibroblasts with FAK showed that all cells had a punctate expression of the protein around their periphery and below their nuclei. However, there was extensive accumulation around the pegs (Fig. 4C, cell labeled *x*), but cells that were not attached to pegs showed significantly less FAK accumulation (cell labeled *y*). Microtubules were visualized immunohistochemically with a tubulin antibody, and nuclei were observed with DAPI stain (Fig. 4D). Microscopy showed that fibroblast nuclei were located centrally when cultured on flat surfaces but moved very close to the pegs and often became distorted after cell attachment to a peg (Fig. 4D). The microtubules also showed a strong eccentric distribution in fibroblasts attached to a peg.

**Reactive forces and fibroblast proliferation.** We hypothesized that fibroblast proliferation depended on either the vertical topography itself or the action-reaction force pairs that exist between two objects as governed by Newton's third law. Newton's third law states that for every action (force), there is an equal and opposite reaction. This means that a cell moving against or attached to a vertical peg would experience a force, and this would be consequently exerted on the cell membrane and transmitted to the rest of the cell via the cytoskeleton. Phase images are shown of fibroblasts plated on an unmodified polystyrene dish after 24 h of culture (Fig. 5A), a dish modified with the addition of unbound mobile microspheres (Fig. 5B), or a dish modified with immobile spheres (Fig. 5C). Fibroblasts can move the mobile microspheres around. On dishes with immobile spheres, fibroblasts migrated until a sphere was contacted and then attached to it much as the fibroblasts did to the pegged structures. The percentage of cells on dishes with mobile spheres was not significantly different from those cultured on flat dishes at 24 h (Fig. 5D). However, on dishes with immobile spheres there was a significant 35% reduction in cell number compared with flat dishes ( $P < 0.05$ ). These experiments were performed to examine whether the presence of microtopography alone could inhibit cell proliferation or whether reactive forces were also important.



*Control of fibroblast cell proliferation in myocyte cultures.* Control of overgrowth of rapidly proliferating nonmyocytes (mainly fibroblasts) is a problem in cardiac cell culture. Therefore, we compared the effectiveness of pegged membranes in reducing the hyperplasia of the remaining fibroblasts in myocyte cultures from a commonly used DNA replication inhibitor, AraC (Fig. 6). After 4 days of culture, total DNA was measured (Fig. 6A) and found to be 37% lower on pegged membranes compared with flat ones ( $P < 0.01$ ,  $n = 4$  cultures). DNA replication was further reduced in the presence of AraC. These results are substantiated by images of cells stained to show the contractile proteins actin and myosin as well as the cell nuclei (Fig. 6, B–E). The conditions used during staining ensured that actin was only visible in the striated myocytes. In this way nonmyocytic cells could be distinguished.

The ratio of fibroblasts to myocytes was estimated by using antibodies specific for myosin heavy chain, which is expressed only in myocytes, and antibodies specific for the aminopropeptide of collagen, which is produced by fibroblasts. A typical Western blot of myocyte myosin and fibroblast aminopropeptide of collagen is shown in Fig. 7A and quantified in Fig. 7, B and C. There was a significant increase in the amount of myosin when cells on flat membranes were treated with AraC (Fig. 7B). Myosin protein was not significantly different between myocytes cultured on pegs with AraC and those cultured on the pegs alone. The protein level of the aminopropeptide of collagen was significantly decreased on pegged membranes compared with flat ones (Fig. 7C). However, in the presence of AraC, collagen was undetectable in cells from both flat and pegged membranes. There was a significant 50% decrease in the ratio of aminopropeptide of collagen to myosin on pegged membranes compared with flat ones (Fig. 7D). Thus on pegged membranes there is a lower ratio of fibroblasts to myocytes after 4 days of culture.

*Connexin43 expression and microtopography.* We hypothesized that the reduction in fibroblast number on pegged membranes might alter myocyte-myocyte interactions and communication. A typical Western blot of connexin43 is shown in Fig. 8A. After 4 days of culture, connexin43 protein levels were measured from cells cultured on flat or pegged membranes (Fig. 8B), and a significant 40% increase on pegged membranes compared with flat ones was found ( $P < 0.05$ ).

## DISCUSSION

We have presented here the finding that a novel microtopography with immovable pegs can alter gene

Fig. 5. Cell proliferation on microtopography with mobile or immobile microspheres. A: fibroblasts cultured on a flat polystyrene petri dish. B: fibroblasts on a flat petri dish with mobile 10-μm polystyrene spheres. C: fibroblasts on a flat petri dish with immobilized 10-μm polystyrene spheres. D: proliferation of fibroblasts after 24 h of culture on the 3 surfaces shown in A–C. There was no difference in cell number between cells cultured on a flat surface and on mobile spheres. There was a significant difference in cell number between those cultured on mobile and immobile spheres. \*\* $P < 0.05$ , flat vs. immobile spheres. Values are means  $\pm$  SE;  $n = 3$  cultures.

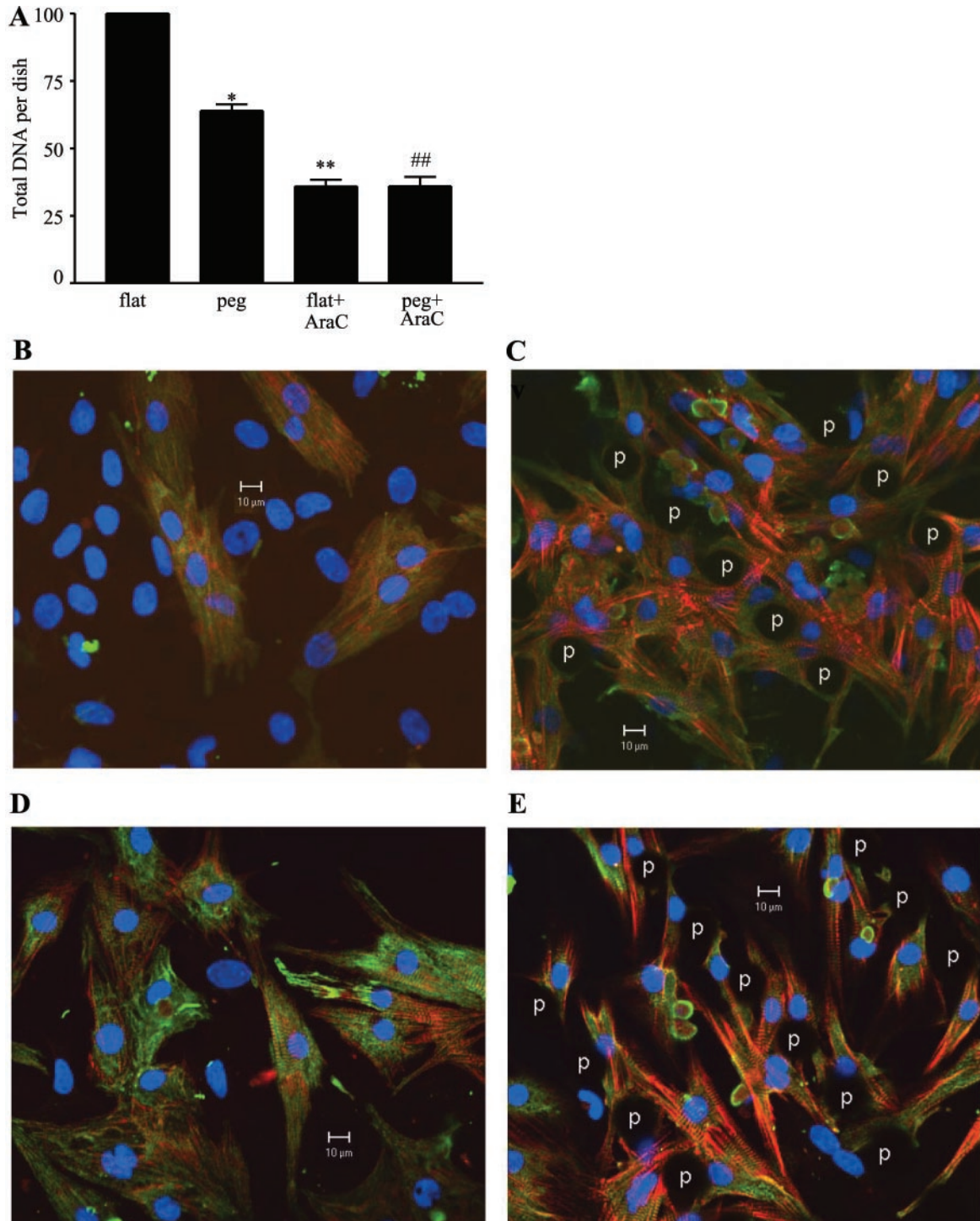


Fig. 6. Effect of microtopography and cytosine  $\beta$ -D-arabino-furanoside (AraC), a cytostatin, on nonmyocyte proliferation in primary cultures from rat neonatal heart. **A**: total DNA isolated from cells in culture 4 days was 37% lower per dish on pegged membranes compared with flat ones (\* $P < 0.01$ , flat vs. peg). In the presence of AraC, DNA replication was further reduced (\*\* $P < 0.01$ , flat vs. flat + AraC; ## $P < 0.01$ , peg vs. peg + AraC). Values are means  $\pm$  SE;  $n = 4$  cultures. **B–E**: primary cardiac cultures stained for nuclei with DAPI (blue), for myosin with MF-20 (green), and for actin with phalloidin (red). Cells are seen growing on a flat membrane without AraC (**B**), a pegged membrane without AraC (**C**), a flat membrane with AraC (**D**), and a pegged membrane with AraC (**E**). Note that in **B** there are many fibroblasts with blue nuclei but with hardly discernable actin staining.

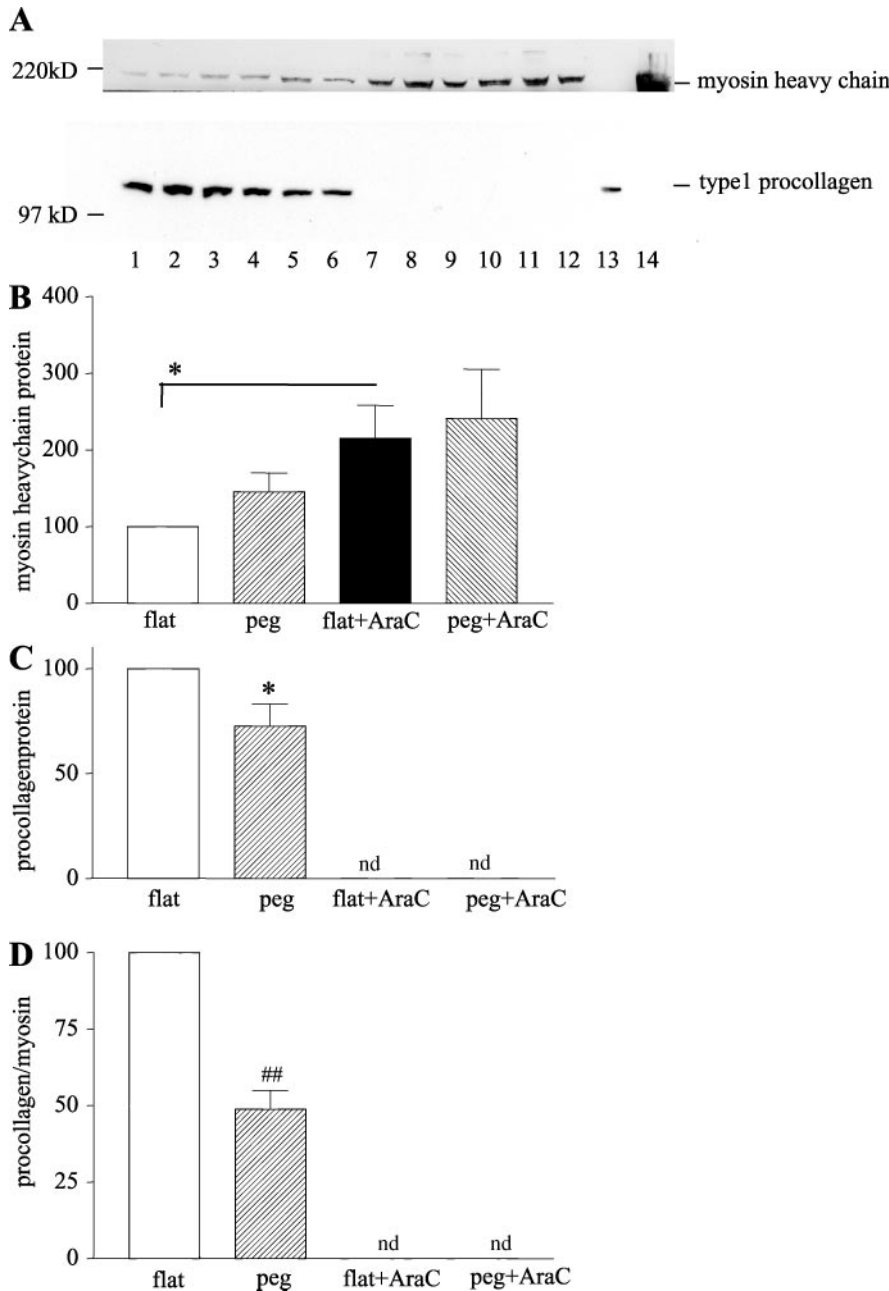


Fig. 7. A: Western blot of myosin and aminopropeptide of collagen. Lanes 1–3, cells cultured on flat membranes; lanes 4–6: cells cultured on pegged membranes; lanes 7–9: cells cultured on flat membranes with AraC; lanes 10–12: cells cultured on pegged membranes with AraC; lane 13: fibroblasts only; and lane 14: a left ventricle from an adult rat heart. B: total myosin heavy chain from the 4 experimental groups. \* $P < 0.05$ , flat vs. flat + AraC. Values are means  $\pm$  SE;  $n = 5$  cultures. C: total aminopropeptide of collagen on flat, pegged, and AraC-treated membranes. \* $P < 0.05$ , flat vs. peg. In the presence of AraC, collagen protein was not detectable. Values are means  $\pm$  SE;  $n = 5$  cultures; nd refers to a value that was below detection level. D: ratio of procollagen to myosin. There is a significant difference between cells cultured on flat membranes and cells cultured on pegged ones ( $## P < 0.01$ ). Values are means  $\pm$  SE;  $n = 5$  cultures; nd refers to a ratio that could not be calculated because collagen detection levels were too low.

expression in rat cardiac fibroblast and myocyte cultures. We also have shown that inhibition of cell proliferation can occur by non-cell-to-cell-mediated mechanisms, namely, the reactive force on the cell when it meets a vertical topographic surface. Fibroblasts cultured in gel matrices that also provide a 3-D environment appear to respond according to the nature of the extracellular matrix to which they are exposed. For example, collagen gels appear to inhibit fibroblast proliferation, whereas 3-D tissue-derived matrices increased their proliferation (7). In our experiments, inhibition of cell proliferation occurred in the absence of an added extracellular matrix and, taken with the findings of the mobile microsphere experiments, suggest that microforces also play an important role in the

process. Cellular attachment to pegs inhibited fibroblast proliferation and was associated with a decreased expression of cyclin D<sub>1</sub> protein, suggesting a G<sub>1</sub>/S<sub>1</sub> cell cycle arrest in these fibroblasts (16). These measurements were taken at a time when cell density on both surfaces was similar so that the only difference was the presence of microtopography. This vertical attachment to pegs appears to be focal adhesion dependent, because inhibition of Rho kinase significantly reduced cellular attachment. A similar inhibition of cell proliferation was also observed with 10- $\mu$ m immobile spheres but was limited if the spheres were free to move. The role of a physical mechanism to inhibit cell division is a novel finding that has not been previously reported and may contribute to the well-known molec-

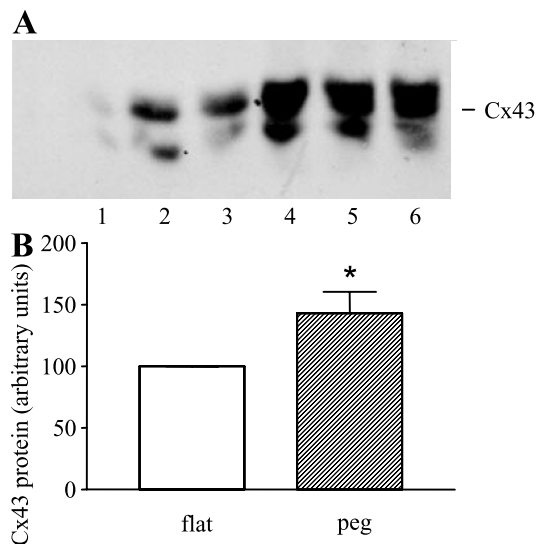


Fig. 8. A: Western blot of connexin43 (Cx43) from primary myocyte cultures grown on flat (lanes 1–3) or pegged membranes (lanes 4–6). B: Cx43 protein expression in cardiac cultures on flat and pegged membranes. Cx43 expression was significantly increased on pegged vs. flat membranes in the absence of AraC (\* $P < 0.05$ ). Values are means  $\pm$  SE;  $n = 4$  cultures.

ular cell-cell interactions. We have taken advantage of this new phenomenon to enrich myocyte cultures by inhibiting fibroblast overgrowth with pegs without the use of pharmacological agents.

The mechanism of contact inhibition has been previously attributed to an interaction of plasma membrane glycoproteins such as gangliosides with membrane receptor protein tyrosine phosphatases on an adjacent cell (25). Plasma membrane gangliosides are also known to be lost in transformed cancer cells (29). In addition to activation of receptor protein tyrosine phosphatases, cell-cell contact is thought to activate a protein called contactinhibin, which in turn inhibits mitogenic pathways (25, 37). These targeted mitogenic pathways are thought to be associated with receptor protein tyrosine kinase and integrin-activated kinases (23, 34). Our findings in this study cannot be explained by the traditional view that contact inhibition is initiated by proteins on adjacent cells because the silicone pegs or polystyrene microspheres are synthetic and inert.

We demonstrate here that fibroblasts attached to pegs often experience distortion of the nucleus. This distortion of the nucleus in response to the reactive forces from the immovable topography may present one mechanism by which fibroblasts alter their proliferation in response to the pegs. Mechanical transduction of force from the extracellular matrix is transmitted to the cytoskeleton through integrins (36). This can lead to displacement of internal organelles, including deformation of the nucleus (18). In chondrocytes, changes to nuclear shape and volume in response to mechanical compressive forces are also mediated by the cytoskeleton (14).

FAK is a tyrosine kinase known to localize to sites of cellular attachment at the focal adhesions (31) and has

been associated with both cell motility and survival. Our study shows that the highest FAK expression is localized around the region of adhesion to the peg. In our model, this is associated with restricted motility following cell attachment as observed by time-lapse video microscopy. The increased concentration of FAK near the peg is also associated with reduced cell proliferation. These data are in contrast to earlier findings that have associated FAK with increased DNA synthesis and  $G_1/S_1$  transition (5). However, FAK-negative cells do not show reduced proliferation, suggesting the role of FAK is more complex than has been previously suggested (17). Our results show that inhibition of Rho kinase reduces cellular attachment to the microtopography. It is known that focal adhesion and stress fiber formation is induced by the Rho family of G proteins (10). Rho targets a number proteins, of which Rho kinase (ROCK) is the best studied. After activation by Rho-GTP, ROCK is able to phosphorylate the myosin-binding subunit of myosin light chain (11). This process is thought to be important in the regulation of focal adhesion formation by ROCK. Our data clearly implicate the Rho signaling pathway as being important in the attachment of fibroblasts to vertical microtopography.

After we observed that fibroblast proliferation was reduced on pegged membranes, we sought to determine whether this could alter fibroblast number in primary myocyte cultures. Myocytes contribute to  $\sim 75\%$  of myocardial size but make up only about one-third of total myocardial cell number (21). Over 90% of these nonmyocytes are thought to be fibroblasts (3) in the myocardium. These fibroblasts secrete most of the extracellular matrix within the myocardium, producing a 3-D network of interacting cells. They play an important physiological role in regulating the activities of myocytes in vivo. Cardiac fibroblasts can modulate the beating frequency of myocytes (27), alter the hypertrophic response of myocytes to growth factors (30) and to mechanical load (38), and change the distribution of extracellular matrix components to influence cardiac development (4) and remodeling (26). The physiological importance of the nonmyocytes in the myocardium cannot be overstated. Yet, in primary neonatal cultures, the nonmyocytes will overgrow the nondividing myocytes without intervention. Our data show that fibroblast proliferation in myocyte cultures is significantly inhibited by the presence of the microtopography.

The proliferation of nonmyocytes, mainly fibroblasts, can also obscure the interpretation of in vitro experiments so that neonatal cultures are usually treated with bromodeoxyuridine (BrdU) (33) or AraC (6). We have shown that the addition of AraC increases the proportion of myosin protein in myocyte cultures due to removal of fibroblast proteins, which dilute the myosin present. Although these compounds reduce nonmyocytic proliferation, they have a number of undesired side effects on myocytes. BrdU is known to depress myocyte contractility (22), and AraC induces apoptosis (12, 19).

Our data show that total DNA isolated from cells cultured on untreated pegged membranes was reduced compared with that from untreated flat membranes. This was accompanied by an increase in the ratio of myocyte-specific myosin to fibroblast procollagen and an increase in connexin43 protein expression. These data strongly suggest that our culture model increases the ratio of myocytes to fibroblasts, allowing more myocyte-myocyte interactions, without pharmacological intervention.

In conclusion, we present a culture model in which the microscale spatial arrangement of vertical silicone pegs provides a novel 3-D environment for cellular attachment in vitro. We show that cell proliferation can be inhibited when a cell meets an inert immovable object in the absence of an added extracellular matrix. This inhibition leads to a similar response that a cell performs when another cell is encountered. We also demonstrate that the Rho signaling pathway plays an important role in this process. The use of silicone gives the potential for studies of mechanical strain in this model of cell culture. The control of nonmyocyte proliferation in vitro may ultimately be useful for tissue engineering applications in vivo.

We appreciate the helpful discussions with Dr. Allen Samarel and the use of the video recording instrumentation kindly provided by Dr. Andrew Maniotis. The MF20 myosin antibody (Fischman) and SP1.D8 (Furthmayr) were obtained from the Developmental Studies Hybridoma Bank under the auspices of the NICHD, maintained by University of Iowa (Biological Sciences, Iowa City, IA 52242).

This research was supported by National Heart, Lung, and Blood Institute Grants HL-64956 and HL-62426 to B. Russell and National Science Foundation Career Grant BES 9983840 to T. A. Desai.

## REFERENCES

- Boateng S, Lateef SS, Crot CA, Motlagh D, Desai TA, Samarel AM, Russell B, and Hanley L. Peptides bound to silicone membranes and 3D microfabrication for cardiac culture. *Adv Mater* 14: 461–463, 2002.
- Boateng SY, Seymour AM, Bhutta NS, Dunn MJ, Yacoub MH, and Boheler KR. Sub-antihypertensive doses of ramipril normalize sarcoplasmic reticulum calcium ATPase expression and function following cardiac hypertrophy in rats. *J Mol Cell Cardiol* 30: 2683–2694, 1998.
- Booz GW and Baker KM. Molecular signalling mechanisms controlling growth and function of cardiac fibroblasts. *Cardiovasc Res* 30: 537–543, 1995.
- Borg TK, Gay RE, and Johnson LD. Changes in the distribution of fibronectin and collagen during development of the neonatal rat heart. *Coll Relat Res* 2: 211–218, 1982.
- Cary LA and Guan JL. Focal adhesion kinase in integrin-mediated signaling. *Front Biosci* 4: D102–D113, 1999.
- Clark WA, Decker ML, Behnke-Barclay M, Janes DM, and Decker RS. Cell contact as an independent factor modulating cardiac myocyte hypertrophy and survival in long-term primary culture. *J Mol Cell Cardiol* 30: 139–155, 1998.
- Cukierman E, Pankov R, Stevens DR, and Yamada KM. Taking cell-matrix adhesions to the third dimension. *Science* 294: 1708–1712, 2001.
- Deutsch J, Motlagh D, Russell B, and Desai TA. Fabrication of microtextured membranes for cardiac myocyte attachment and orientation. *J Biomed Mater Res* 53: 267–275, 2000.
- Dunn JC, Yarmush ML, Koebe HG, and Tompkins RG. Hepatocyte function and extracellular matrix geometry: long-term culture in a sandwich configuration. *FASEB J* 3: 174–177, 1989.
- Geiger B and Bershadsky A. Assembly and mechanosensory function of focal contacts. *Curr Opin Cell Biol* 13: 584–592, 2001.
- Geiger B and Bershadsky A. Exploring the neighborhood: adhesion-coupled cell mechanosensors. *Cell* 110: 139–142, 2002.
- Grant S. Ara-C: cellular and molecular pharmacology. *Adv Cancer Res* 72: 197–233, 1998.
- Green AM, Jansen JA, van der Waerden JP, and von Recum AF. Fibroblast response to microtextured silicone surfaces: texture orientation into or out of the surface. *J Biomed Mater Res* 28: 647–653, 1994.
- Guilak F. Compression-induced changes in the shape and volume of the chondrocyte nucleus. *J Biomech* 28: 1529–1541, 1995.
- Haddad J, Decker ML, Hsieh LC, Lesch M, Samarel AM, and Decker RS. Attachment and maintenance of adult rabbit cardiac myocytes in primary cell culture. *Am J Physiol Cell Physiol* 255: C19–C27, 1988.
- Huang S, Chen CS, and Ingber DE. Control of cyclin D1, p27(Kip1), and cell cycle progression in human capillary endothelial cells by cell shape and cytoskeletal tension. *Mol Biol Cell* 9: 3179–3193, 1998.
- Ilic D, Furuta Y, Kanazawa S, Takeda N, Sobue K, Nakatsuji N, Nomura S, Fujimoto J, Okada M, and Yamamoto T. Reduced cell motility and enhanced focal adhesion contact formation in cells from FAK-deficient mice. *Nature* 377: 539–544, 1995.
- Janmey PA. The cytoskeleton and cell signaling: component localization and mechanical coupling. *Physiol Rev* 78: 763–781, 1998.
- Kufe DW and Spriggs DR. Biochemical and cellular pharmacology of cytosine arabinoside. *Semin Oncol* 12: 34–48, 1985.
- Lateef SS, Boateng S, Hartman TJ, Crot CA, Russell B, and Hanley L. GRGDSP peptide-bound silicone membranes withstand mechanical flexing in vitro and display enhanced fibroblast adhesion. *Biomaterials* 23: 3159–3168, 2002.
- Lijnen P and Petrov V. Renin-angiotensin system, hypertrophy and gene expression in cardiac myocytes. *J Mol Cell Cardiol* 31: 949–970, 1999.
- Lokuta A, Kirby MS, Gaa ST, Lederer WJ, and Rogers TB. On establishing primary cultures of neonatal rat ventricular myocytes for analysis over long periods. *J Cardiovasc Electro-physiol* 5: 50–62, 1994.
- Meuillet EJ, Kroes R, Yamamoto H, Warner TG, Ferrari J, Mania-Farnell B, George D, Rebbaa A, Moskal JR, and Bremer EG. Sialidase gene transfection enhances epidermal growth factor receptor activity in an epidermoid carcinoma cell line, A431. *Cancer Res* 59: 234–240, 1999.
- Nagatoya K, Moriyama T, Kawada N, Takeji M, Oseto S, Murozono T, Ando A, Imai E, and Hori M. Y-27632 prevents tubulointerstitial fibrosis in mouse kidneys with unilateral ureteral obstruction. *Kidney Int* 61: 1684–1695, 2002.
- Nelson PJ and Daniel TO. Emerging targets: molecular mechanisms of cell contact-mediated growth control. *Kidney Int* 61, Suppl 1: 99–105, 2002.
- Ogawa E, Saito Y, Harada M, Kamitani S, Kuwahara K, Miyamoto Y, Ishikawa M, Hamanaka I, Kajiyama N, Takahashi N, Nakagawa O, Masuda I, Kishimoto I, and Nakao K. Outside-in signalling of fibronectin stimulates cardiomyocyte hypertrophy in cultured neonatal rat ventricular myocytes. *J Mol Cell Cardiol* 32: 765–776, 2000.
- Orita H, Fukasawa M, Hirooka S, Uchino H, Fukui K, and Washio M. Modulation of cardiac myocyte beating rate and hypertrophy by cardiac fibroblasts isolated from neonatal rat ventricle. *Jpn Circ J* 57: 912–920, 1993.
- Perhonen M, Sharp WW, and Russell B. Microtubules are needed for dispersal of alpha-myosin heavy chain mRNA in rat neonatal cardiac myocytes. *J Mol Cell Cardiol* 30: 1713–1722, 1998.
- Rosner H, Greis C, and Rodemann HP. Density-dependent expression of ganglioside GM3 by human skin fibroblasts in an all-or-none fashion, as a possible modulator of cell growth in vitro. *Exp Cell Res* 190: 161–169, 1990.

30. **Sadoshima J and Izumo S.** Molecular characterization of angiotensin II-induced hypertrophy of cardiac myocytes and hyperplasia of cardiac fibroblasts. Critical role of the AT1 receptor subtype. *Circ Res* 73: 413–423, 1993.
31. **Schaller MD.** Biochemical signals and biological responses elicited by the focal adhesion kinase. *Biochim Biophys Acta* 1540: 1–21, 2001.
32. **Schmidt JA and von Recum AF.** Surface characterization of microtextured silicone. *Biomaterials* 13: 675–681, 1992.
33. **Simpson P and Savion S.** Differentiation of rat myocytes in single cell cultures with and without proliferating nonmyocardial cells. Cross-striations, ultrastructure, and chronotropic response to isoproterenol. *Circ Res* 50: 101–116, 1982.
34. **Slevin M, Kumar S, He X, and Gaffney J.** Physiological concentrations of gangliosides GM1, GM2 and GM3 differentially modify basic-fibroblast-growth-factor-induced mitogenesis and the associated signalling pathway in endothelial cells. *Int J Cancer* 82: 412–423, 1999.
35. **Van Kooten TG, Whitesides JF, and von Recum A.** Influence of silicone (PDMS) surface texture on human skin fibroblast proliferation as determined by cell cycle analysis. *J Biomed Mater Res* 43: 1–14, 1998.
36. **Wang N, Tolic-Norrelykke IM, Chen J, Mijailovich SM, Butler JP, Fredberg JJ, and Stamenovic D.** Cell prestress. I. Stiffness and prestress are closely associated in adherent contractile cells. *Am J Physiol Cell Physiol* 282: C606–C616, 2002.
37. **Wieser RJ, Renauer D, Schafer A, Heck R, Engel R, Schutz S, and Oesch F.** Growth control in mammalian cells by cell-cell contacts. *Environ Health Perspect* 88: 251–253, 1990.
38. **Wollert KC and Drexler H.** The renin-angiotensin system and experimental heart failure. *Cardiovasc Res* 43: 838–849, 1999.

